Electronic Supplementary Material (ESI) for Journal of Materials Chemistry C.


# Supporting Information
# for
# $Ti_3C_2T_x$ Quantum Dots/ Polyvinyl alcohol Films as Enhanced Long-term Stable Saturable Absorber Device for Ultrafast Photonics

Jianfeng Liu[1], Shanshan Chen[1,2]*, Lili Tao[1,2], Yu Zhao[1,2], Junshan He[1], Le Huang[1,2], Yibin Yang[1,2]

[1]*School of Materials and Energy, Guangdong University of Technology, Guangzhou, 510006, China*

[2]*Guangdong Provincial Key Laboratory of Information Photonics Technology, Guangdong University of Technology, Guangzhou, 510006, China*

*Corresponding author: chensunny@gdut.edu.cn*

## Preparation of $Ti_3C_2T_x$ QDs and its PVA SA Device

Firstly, the mixture of 3.2 g lithium fluoride (99.99 %, Macklin) and 40 mL 9 M hydrochloric acid (36 wt%, Guangzhou) was served as the etchant to obtain $Ti_3C_2T_x$ NSs. Magnetic stirrer was exploited to ensure the mixture complete dissolution in a 100 ml polytetrafluoroethylene beaker. Then, 2.0 g $Ti_3AlC_2$ (400 mesh, 11 Technology Co., Ltd., China) was slowly added to the solvent. The etching procedure was stirred at 350 rpm for 24 h at 35℃. Next, 1 M HCl was used to remove excess LiF and coproduct $AlF_3$ by centrifugation (H1850, Cence, China) for 2-3 times after reaction. Subsequent wash with deionized water for several times to make the pH of the supernatant reach 6, and then the multilayer $Ti_3C_2T_x$ was obtained. Better delamination was carried by an ice bath ultrasonication (KQ-500VDE, ShuMei) for 2 hours until the sediment swelling. The mono or few-layer $Ti_3C_2T_x$ in dark green supernatant was collected by repeatedly centrifuging at 3500 rpm for 1 h. the dehydration process was conducted in a freezing dryer (LC-12N-50A, LiChen) to keep the mono or few-layer $Ti_3C_2T_x$ from oxidization. A portion of the fully dried mono or few-layer $Ti_3C_2T_x$ was used for characterization, and the remaining portion was used to prepare quantum dots by probe sonication (Scientz-II, SCIENTZ, Ningbo Scientz Biotechnology Co., Ltd.) in ethanol (99.7%, Sun, Tianjin Zhiyuan Reagent Co., Ltd) for 12 hours. Finally, $Ti_3C_2T_x$ QDs was collected by centrifugation for twice at 10000 rpm for 1 h and distilled to 10 ml.

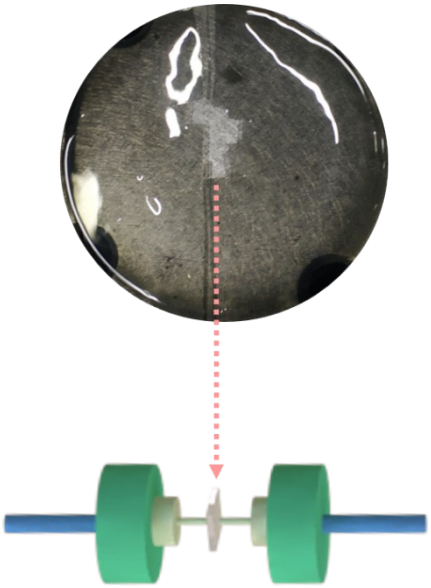

**Figure S1** Schematic diagram of $Ti_3C_2T_x$ QDs/PVA SA device.

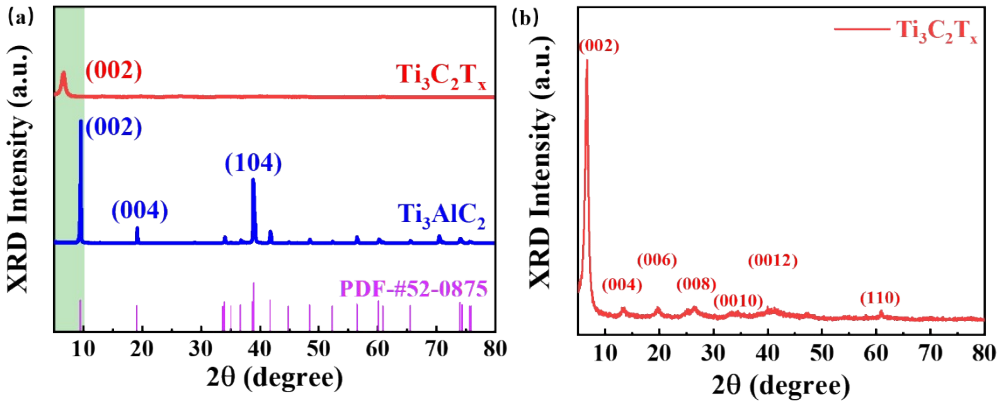


**Figure S2** (a) XRD patterns of $Ti_3AlC_2$ MAX, $Ti_3C_2T_x$ NSs. (b) XRD pattern of $Ti_3C_2$Tx NSs.

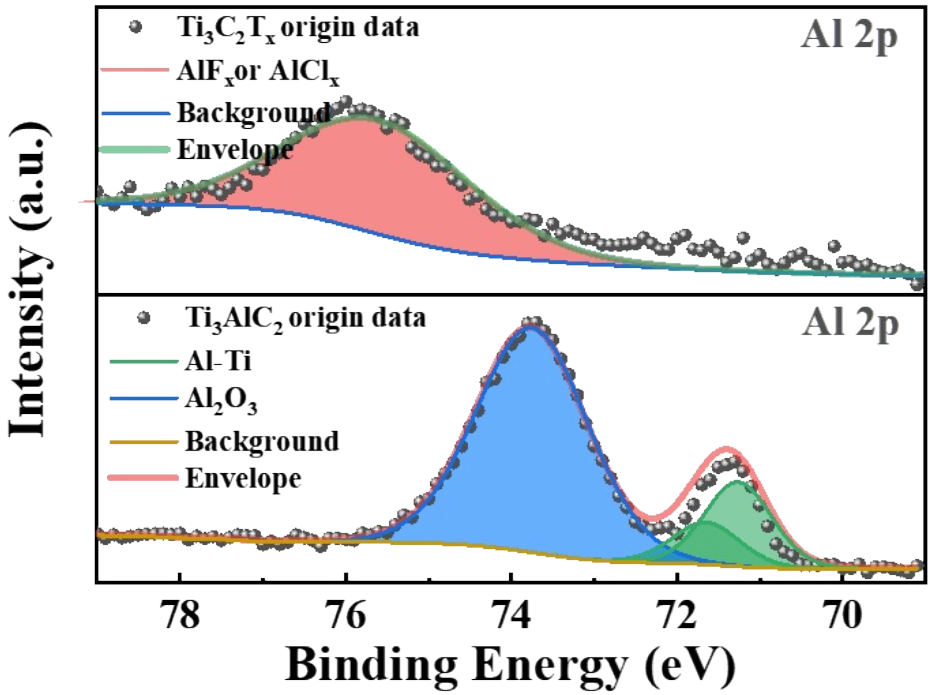


**Figure S3** Component peak-fitting of XPS spectra for Al

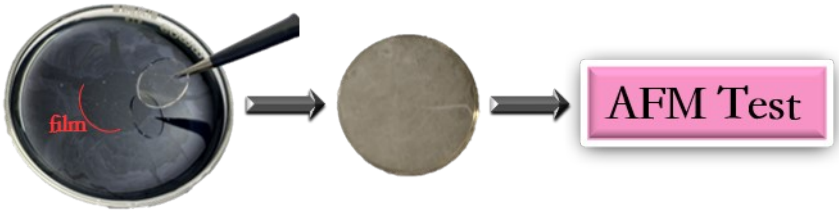


**Figure S4** Schematic diagram of SPM test method.

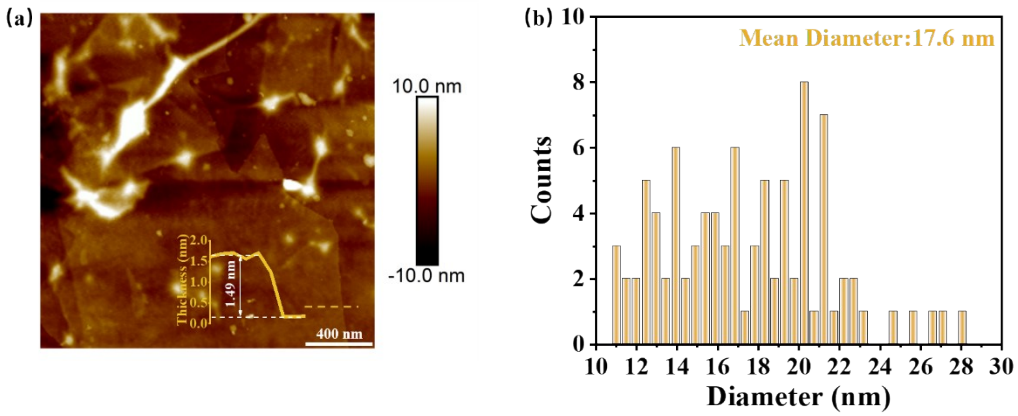


**Figure S5** (a) SPM image of $Ti_3C_2T_x$ NSs. (b) Diameter histogram of $Ti_3C_2T_x$ QDs.

## Ultrafast Laser Application

The ring cavity was pumped by a 980 nm single-mode diode laser (Connet, VLSS-980) with a 980/1550 nm wavelength division multiplexer (WDM). A 1.2 m $Er^{3+}$ doped fiber (EDF, LIEKKI, Er30) was used as the gain medium. The polarization independent isolator (PI-ISO) was employed to ensure the unidirectional operation of the laser in the ring cavity. Cavity polarization state and intracavity birefringence were adjusted by a polarization controller (PC). The PVA SA based on $Ti_3C_2T_x$ QDs was incorporated between WDM and PC through FC (Ferrule Contactor)/APC (Angled Physical Contact) connectors. 10% of the laser separated by the OC (9:1) was used for detection, and the remaining 90% returned ring cavity to continue resonance. In addition, a certain length of single-mode fiber (SMF) was needed to the ring cavity for signal output. The output laser characteristics were monitored by an oscilloscope (Tektronix, MDO4104B) equipped with an ultrafast photodetector (EOT, ET-5000). The output laser spectrum was detected by an optical analyzer (Avesta.ASP-IR-2.6). The width of mode-locked pulse was detected by an autocorrelator (Femtochrome, FR-103XL).

The group velocity dispersion (GVD) of EDF and SMF were 21.7 $ps^2$/km and -27.6 $ps^2$/km at 1550 nm, respectively. In the mode-locked case, the cavity length was 22.6 m. Therefore, when the dispersion of PVA SA or other influence factors was not considered, the net dispersion could be calculated to be -0.565 $ps^2$ for mode-locked laser. It means the EDFL operated in an anomalous region.

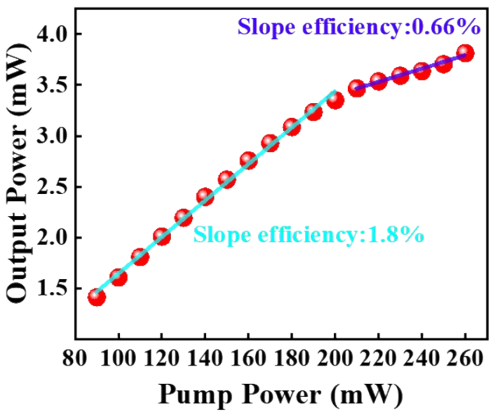


**Figure S6** Output power varies with pump power. (Q-switched)

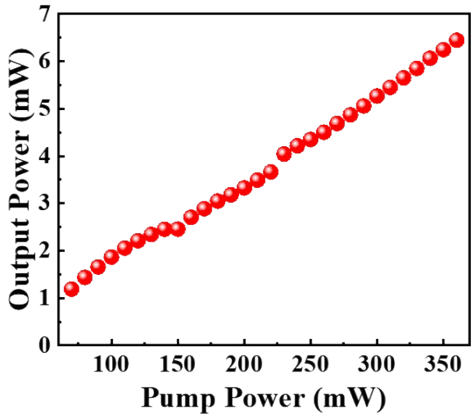


**Figure S7** Output power varies with pump power. (Mode-locked)

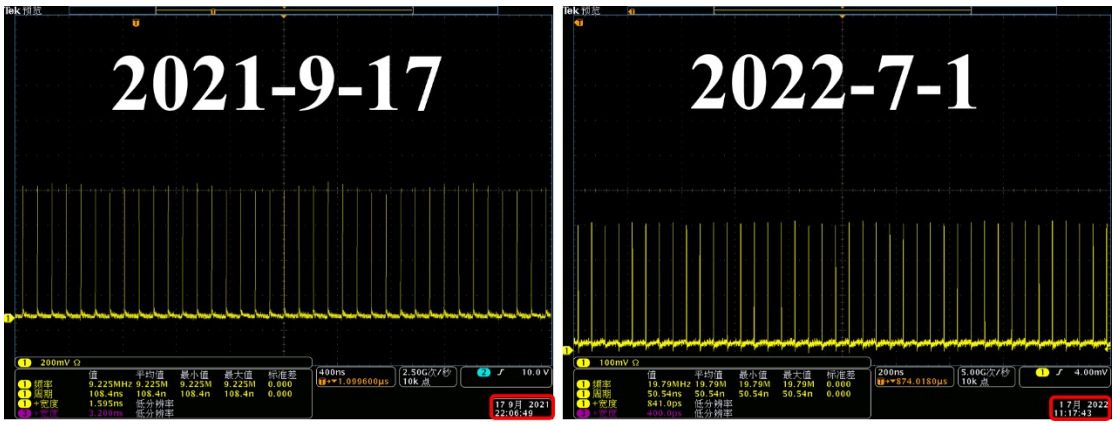


**Figure S8** Oscilloscope screenshots of the mode-locking operation based on $Ti_3C_2T_x$ QDs at different times.

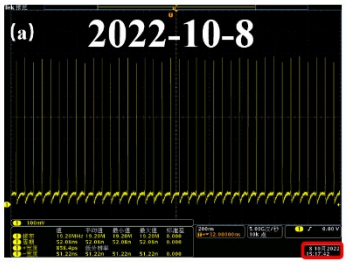
(a)
2022-10-8

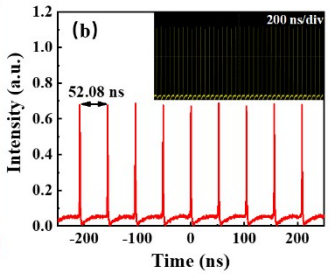
(b)
200 ns/div
52.08 ns
Intensity (a.u.)
Time (ns)

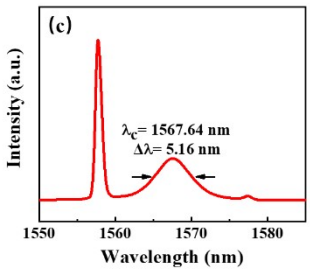
(c)
λc= 1567.64 nm
Δλ= 5.16 nm
Intensity (a.u.)
Wavelength (nm)

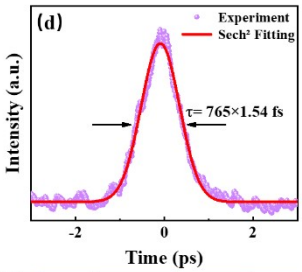
(d)
Experiment
Sech² Fitting
τ= 765×1.54 fs
Intensity (a.u.)
Time (ps)

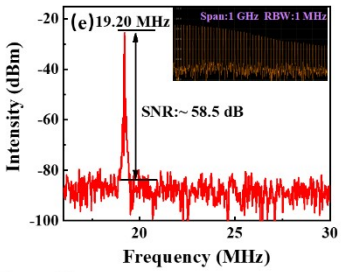
(e)19.20 MHz
Span:1 GHz RBW:1 MHz
SNR:~ 58.5 dB
Intensity (dBm)
Frequency (MHz)

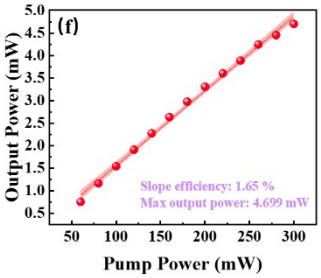
(f)
Slope efficiency: 1.65 %
Max output power: 4.699 mW
Output Power (mW)
Pump Power (mW)

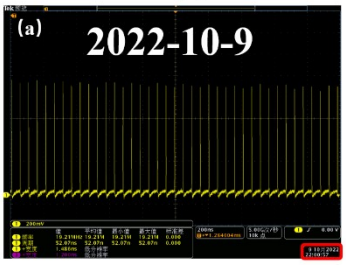
(a)
2022-10-9

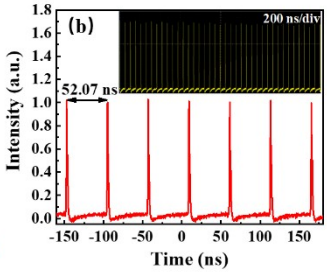
(b)
200 ns/div
52.07 ns
Intensity (a.u.)
Time (ns)

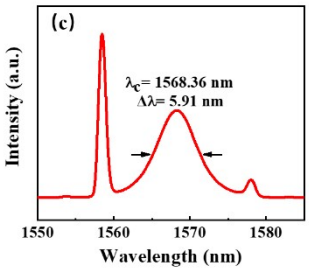
(c)
λc= 1568.36 nm
Δλ= 5.91 nm
Intensity (a.u.)
Wavelength (nm)

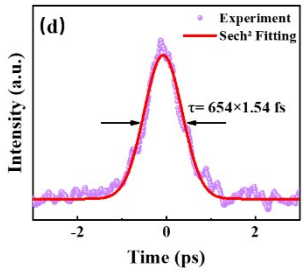
(d)
Experiment
Sech² Fitting
τ= 654×1.54 fs
Intensity (a.u.)
Time (ps)

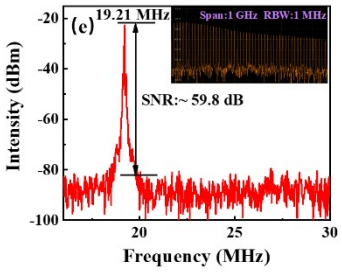
(e)19.21 MHz
Span:1 GHz RBW:1 MHz
SNR:~ 59.8 dB
Intensity (dBm)
Frequency (MHz)

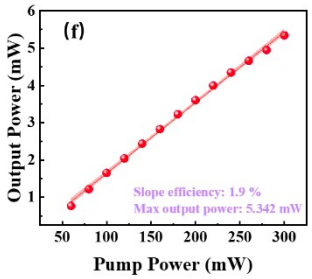
(f)
Slope efficiency: 1.9 %
Max output power: 5.342 mW
Output Power (mW)
Pump Power (mW)

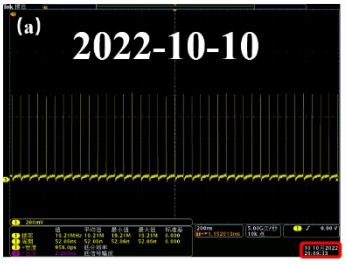
(a)
2022-10-10

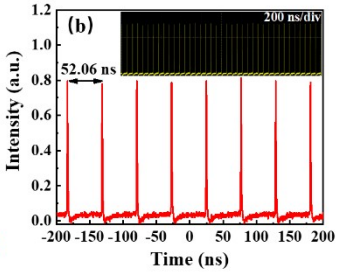
(b)
200 ns/div
52.06 ns
Intensity (a.u.)
Time (ns)

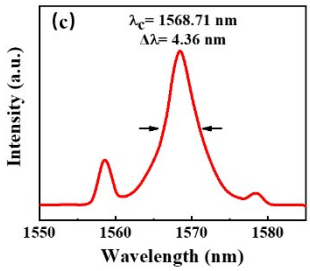
(c)
λc= 1568.71 nm
Δλ= 4.36 nm
Intensity (a.u.)
Wavelength (nm)

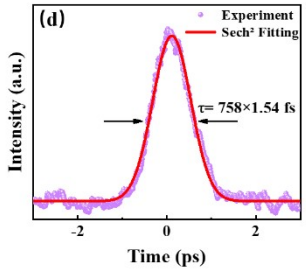
(d)
Experiment
Sech² Fitting
τ= 758×1.54 fs
Intensity (a.u.)
Time (ps)

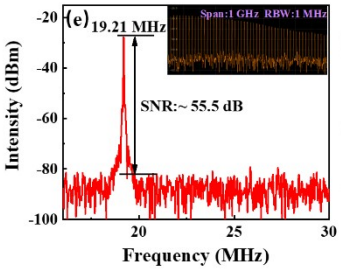
(e)19.21 MHz
Span:1 GHz RBW:1 MHz
SNR:~ 55.5 dB
Intensity (dBm)
Frequency (MHz)

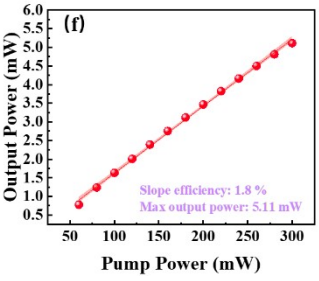
(f)
Slope efficiency: 1.8 %
Max output power: 5.11 mW
Output Power (mW)
Pump Power (mW)

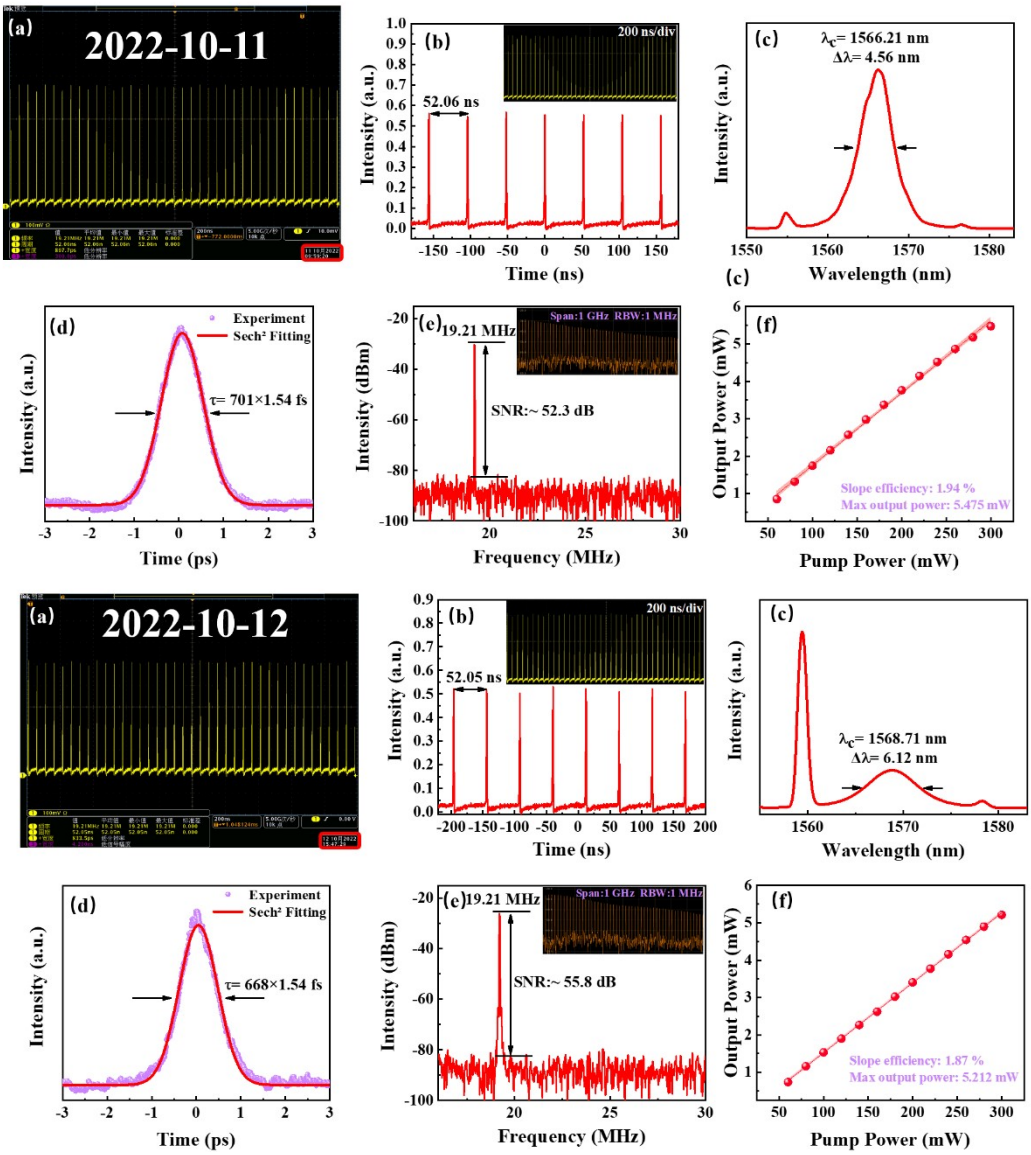


**Figure S9** (a) Oscilloscope screenshots (various days). (b) Pulse sequences. (c) Mode-locking optical spectrum. (d) Autocorrelation trace with a sech$^2$ fitting. (e) The RF spectrum at the fundamental frequency; inset: the broadband RF spectrum withing 1 GHz with a RBW of 1 MHz. (f) Output power varies with pump power.

**Table S1 XPS peak fitting results for as-prepared $Ti_3C_2T_x$.**

| Region | BE (eV) | FWHM (eV) | Fraction (%) | Assigned to |
|---|---|---|---|---|
| Ti $2p_{3/2}$ ($2p_{1/2}$) | 454.7(460.6) | 1.2(2.0) | 45 | C-Ti-C |
| | 455.7(461.5) | 1.5(2.0) | 27 | C–Ti–O |
| | 456.9(462.8) | 2.0(1.3) | 21 | C–Ti–F/Cl |
| | 458.6(464.2) | 1.5(1.6) | 7 | $TiO_2$ |
| C 1s | 281.7 | 0.8 | 46 | C-Ti-C |
| | 282.6 | 0.7 | 6 | C-Ti-$T_x$ |
| | 284.8 | 3.2 | 48 | C-C |
| O 1s | 529.8 | 1.3 | 30 | $TiO_2$ |
| | 531.0 | 1.5 | 40 | C-Ti-$O_x$ |
| | 532.2 | 1.5 | 19 | C-Ti-$(OH)_x$ |
| | 533.4 | 1.5 | 9 | $H_2O$ |
| | 535.0 | 1.5 | 2 | $Al(OF)_x$ |
| F 1s | 684.3 | 1.6 | 47 | C-Ti-F |
| | 686.0 | 2.5 | 53 | Metal fluoride ($AlF_x$) |
| Al 2p | 75.6 | 2.73 | 100 | $AlF_x$ or $AlCl_x$ |
| Cl 2p | 199.1(200.8) | 1.2(1.2) | 78 | C-Ti-Cl |
| | 200.1(201.8) | 1.5(1.5) | 22 | Metal chloride ($AlCl_x$) |

**Table S2 XPS peak fitting results for $Ti_3AlC_2$(MAX).**

| Region | BE (eV) | FWHM (eV) | Fraction (%) | Assigned to |
|---|---|---|---|---|
| Ti $2p_{3/2}$ ($2p_{1/2}$) | 453.9(460.0) | 1.2(1.3) | 25 | C-Ti-C |
| | 455.4(461.3) | 2.5(3.0) | 33 | C-Ti-Al |
| | 458.2(463.9) | 1.5(1.9) | 42 | $TiO_2$ |
| C 1s | 281.0 | 0.8 | 7 | C-Ti |
| | 284.8 | 1.5 | 74 | C-C |
| | 286.4 | 1.5 | 12 | C-O |
| | 288.8 | 1.3 | 7 | C=O |
| O 1s | 529.7 | 1.5 | 39 | $TiO_2$ |
| | 531.6 | 2.4 | 53 | C-Ti-$O_x$ |
| | 533.6 | 1.5 | 8 | $H_2O$ |
| Al $2p_{3/2}$ ($2p_{1/2}$) | 71.3(71.7) | 0.7(0.7) | 19 | Al-Ti |
| | 73.8 | 1.7 | 81 | $Al_2O_3$ |

**Table S3** Summary of performance for five consecutive days.

| Time | Central wavelength / Bandwidth (nm) | Repetition Rate (MHz) | Pulse duration (fs) | SNR (dBm) |
|---|---|---|---|---|
| 2022-10-8 | 1567.64/5.16 | 19.20 | 765 | 58.5 |
| 2022-10-9 | 1568.36/5.91 | 19.21 | 654 | 59.8 |
| 2022-10-10 | 1568.71/4.36 | 19.21 | 758 | 55.5 |
| 2022-10-11 | 1566.21/4.56 | 19.21 | 701 | 52.3 |
| 2022-10-12 | 1568.71/6.12 | 19.21 | 668 | 55.8 |